

Luminescent and Electronic Properties of Stilbenoid NCN-Pincer Pt^{II} Compounds

Guido D. Batema,^[a] Koen T. L. van de Westelaken,^[a] Javier Guerra,^[a] Martin Lutz,^[b] Anthony L. Spek,^[b] Cornelis A. van Walree,^[a] Celso de Mello Donegá,^[c] Andries Meijerink,^[c] Gerard P. M. van Klink,^[a] and Gerard van Koten*^[a]

Keywords: Donor–acceptor systems / Luminescence / N-ligands / Platinum

A series of novel 4,4'-disubstituted organic–organometallic stilbenes were synthesized, that is, the 4'-substituted stilbenoid–NCN-pincer platinum(II) complexes [PtCl(NCN–R-4)] (NCN–R-4 = [C₆H₂(CH₂NMe₂)₂-2,6-R-4][−] in which R = C₂H₂C₆H₄-R'-4' with R' = NMe₂, OMe, SiMe₃, H, I, CN, NO₂) (**1–7**). In these compounds the PtCl grouping can be considered to be present as a donor substituent. Their synthesis involved a Horner–Wadsworth–Emmons reaction of [PtCl(NCN–CHO-4)] (**9**) with the appropriate phosphonate ester derivatives (**8a–g**). Under these reaction conditions, the C–Pt bond in aldehyde **9** was not affected, and the platinated stilbene products were obtained in 53–90% yield. The solid-state structures of complexes **1**, **2** and **5–7** were determined by single-crystal X-ray diffraction, which revealed interesting bent conformations for **2**, **5** and **7**. Linear correlations were found between both the ¹³C{¹H} (C *ipso* to Pt) and the ¹⁹⁵Pt{¹H} NMR chemical shift and the Hammett σ_p value of

the R' substituent; therefore, these NMR shifts can be used as a qualitative probe for the electronic properties of the delocalized π -system to which it is connected. The platinum–stilbene complexes were investigated for charge-transfer properties in solvents of different polarity. The luminescent properties, shown by donor–acceptor complexes **1**, **6** and **7**, were investigated by fluorescence spectroscopy, and the complexes showed positive solvatochromism, which indicates dipolar character of the excited state. The excited state lifetimes, which were in the picosecond range, and the quantum yields (ranging from 0.002 to 0.2) were also determined for these complexes. It was established that the presence of the transition metal favours nonradiative decay from the excited state to the ground state.

(© Wiley-VCH Verlag GmbH & Co. KGaA, 69451 Weinheim, Germany, 2007)

Introduction

Conjugated molecules are regarded with high interest for their optoelectronic properties^[1] in, for instance, materials with nonlinear optical (NLO)^[2] behaviour and for applications in optoelectronic devices such as light-emitting diodes.^[3] The properties of these molecules depend on the nature and length of the conjugation path and on the functional groups present in the system. By connecting donor and acceptor groups through a π -electron bridge, intra-

molecular electron transfer can be achieved. A well-known example of such a push–pull conjugated system is *trans* 4-dimethylamino-4'-nitrostilbene (DANS),^[4] a member of the *trans* 4,4'-disubstituted stilbene family (Scheme 1), which has been studied predominantly for its special photophysical and NLO properties.^[5–8]

Currently, conjugated systems containing transition metals attract much attention,^[9–13] especially because the optoelectronic properties of these systems can be affected by changing the metal ion, the coordinating anions and ligands or by changing the nature of the connecting conjugated system. Interesting examples of metal–organic conjugated molecules studied for their NLO properties are the ferrocene-functionalized donor–acceptor complexes reported by McCleverty and coworkers.^[14–17] In our group, bis(pincer–metal)acetylene complexes^[18–21] and heterometallic terpyridine–pincer-based complexes^[22] were studied in which the communication between two metals by a conjugated ligand bridge was investigated.

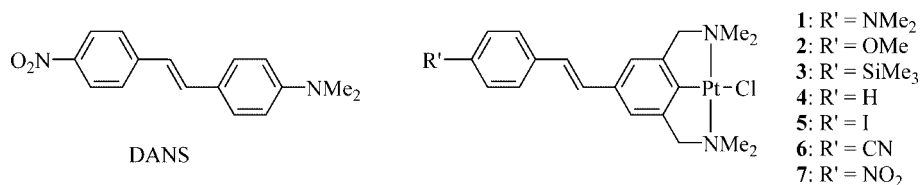
We already showed the feasibility of remotely influencing the electron density on the metal centre of the [MX(NCN–R-4)] pincer system (M = Ni, Pd or Pt; X = Cl, Br or I) by altering the *para* substituent R [R = NO₂, C(O)Me, COOH,

[a] Organic Chemistry and Catalysis, Faculty of Science, Utrecht University, Padualaan 8, 3584 CH Utrecht, The Netherlands
Fax: +31-30-2523615
E-mail: g.vankoten@chem.uu.nl

[b] Crystal and Structural Chemistry, Faculty of Science, Utrecht University, Padualaan 8, 3584 CH Utrecht, The Netherlands

[c] Condensed Matter and Interfaces, Faculty of Science, Utrecht University, P.O. Box 80.000, Princetonplein 1, 3508 TA Utrecht, The Netherlands

Supporting information for this article is available on the WWW under <http://www.eurjic.org> or from the author.



Scheme 1.

CHO, SO₃H, PO(OEt)₂, PO(OH)(OEt), PO(OH)₂, I, Cl, H, CH₂OH, OMe, SMe or NH₂].^[23,24] In this series, a linear correlation was found between the ease of oxidation of the nickel centre and the electron-donating properties of the *para* substituent [redox potential $E_{p,a}$ (Ni^{II}/Ni^{III}) versus σ_p]. Correlations were also found between NMR chemical shifts [¹³C{¹H} and ¹⁹⁵Pt{¹H}] of the complexes and the Hammett substituent parameter σ_p (for M = Ni: $\delta = {}^{13}\text{C}_{\text{ipso}}$ versus σ_p ; for M = Pt: $\delta = {}^{195}\text{Pt}$ versus σ_p). Conversely, in the same study, for the carboxylic acid functionalized platinum compound [PtI(NCN-COOH-4)], the Hammett σ_p value of the platinum iodide moiety was determined to amount to -1.18 in methanol and -0.72 in water/methanol (1:1). The value and the negative sign of this Hammett substituent constant implied that the *para* platinum iodide group can be considered as an electron-donating substituent comparable in strength to a dimethylamino group [NMe₂; $\sigma_p = -0.83$; the tabulated σ_m value of the CH₂N(Me)₂ group is 0.00].^[25] Consequently, it should be possible to introduce the aryl NCN metal system as the donor group into a donor-acceptor system, like in DANS, that is, to replace the *N,N*-dimethylaminobenzene moiety with the NCN-PtCl moiety (Scheme 1). Moreover, recent studies showed that certain Pt^{II}-pincer systems have interesting photochemical properties;^[26–28] for example, Connick and coworkers studied luminescent NCN-Pt^{II} pincer complexes based on 1,3-bis(piperidylmethyl)benzene.^[29–31] Kanbara and coworkers applied a thioamide-based SCS-Pt^{II} pincer complex in a light-emitting diode exhibiting red-coloured electroluminescence.^[32]

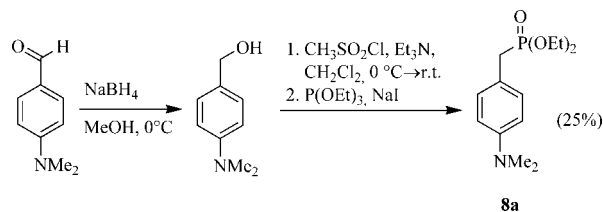
In the present study we set out to prepare a series of stilbenoid platinum compounds [PtCl{NCN(C₂H₂C₆H₄-R'-4')-4}] (1–7) in which the donor site (the PtCl grouping) is kept constant and the nature of the R' group is varied (R' = NMe₂, OMe, SiMe₃, H, I, CN, NO₂). By introducing different substituents at the 4'-position of the stilbenoid-pincer backbone, the donor-acceptor properties of the stilbenoid platinum system could be studied.

An important synthetic objective of the present study was to explore methods for the construction of the stilbene moiety by using a suitable *para*-substituted pincer molecule with the NCN-Pt arrangement already in place. A pronounced influence of the *para* substituent on the (photo)-physical properties of the stilbenoid platinum complexes has been found and will be discussed with the help of the results from solid-state structures, ¹³C{¹H} and ¹⁹⁵Pt{¹H} NMR spectroscopic analysis, UV/Vis and emission spectroscopy.

Results and Discussion

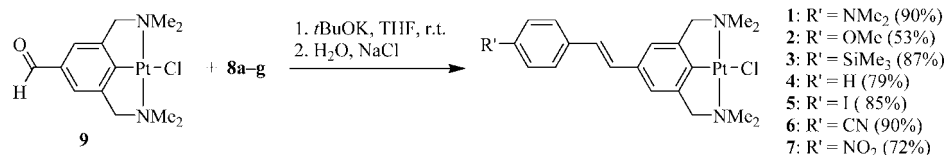
Synthesis

A series of substituted benzyl phosphonates^[33–38] **8b–g** was prepared by a Michaelis–Arbuzov reaction between triethyl phosphite and the appropriate *para*-substituted benzylic bromide, which were either commercially available or could be prepared in a single step by a recently improved^[39] radical bromination reaction of the available toluene derivative. Phosphonate ester **8a** was synthesized by reduction of 4-dimethylaminobenzaldehyde with sodium borohydride to form 4-dimethylaminobenzyl alcohol,^[40] which was then in situ reacted with methanesulfonyl chloride and subsequently converted into the phosphonate ester by an Arbuzov reaction^[41] (Scheme 2).



Scheme 2.

Stilbenoid NCN-pincer platinum(II) compounds **1–7** were obtained as *trans* compounds in moderate-to-good yield by a Horner–Wadsworth–Emmons condensation reaction of [PtCl(NCN-CHO-4)] (**9**) and the appropriate phosphonate ester **8** in the presence of potassium *tert*-butoxide (Scheme 3).^[42–44] Upon hydrolysis of the reaction mixture, the pure *trans* isomers of **1–7** precipitated out of the solution and were isolated by filtration as air-stable solids. The solids were fully characterized by ¹H, ¹³C{¹H} and ¹⁹⁵Pt{¹H} NMR spectroscopy, elemental analysis, mass spectrometry, and compounds **1**, **2**, **5**, **6** and **7** were also characterized by single-crystal X-ray structure determination. In this study, only the *trans* isomers of **1–7** were obtained in a pure form and further studied. From the filtrate, a *trans*–*cis* mixture (determined by ¹H NMR spectroscopy) was obtained of which the *cis* isomer was always present as the minor component. In the solid state, the compounds do not undergo *trans*–*cis* isomerization upon exposure to daylight in contrast to the compounds in solution, which do undergo this *trans*–*cis* isomerization.^[5,6] Noteworthy, the Pt–C bond of **9** remains intact throughout the complete reaction under the applied reaction conditions and no visible formation of zero-valent platinum was ob-



Scheme 3.

served in the olefination reaction induced by the presence of the strong base.

Crystal Structures

Crystals suitable for single-crystal X-ray structure determination of **1** (Figure 1), **2**, **5**, **6** and **7** (Figure 2) were obtained by slow evaporation of deuterated dichloromethane solutions, which were initially prepared and used for the NMR studies.

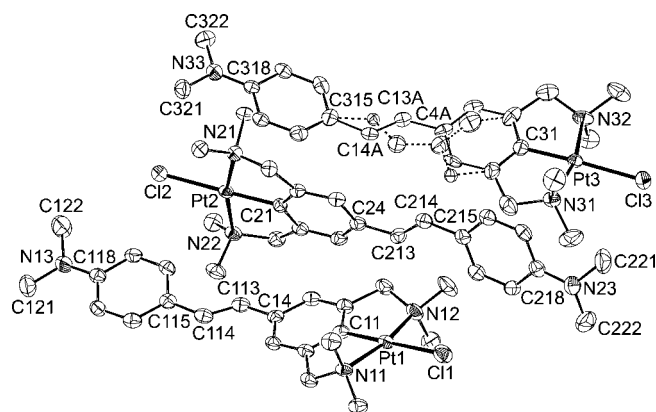


Figure 1. Displacement ellipsoid plot (50% probability level) of the three independent molecules in the crystal structure of **1** (viewed along the crystallographic *b* axis). Hydrogen atoms and partially occupied CH₂Cl₂ molecules are omitted for clarity. The minor conformation (19% occupancy) of disordered residue 3 is drawn in dashed lines.

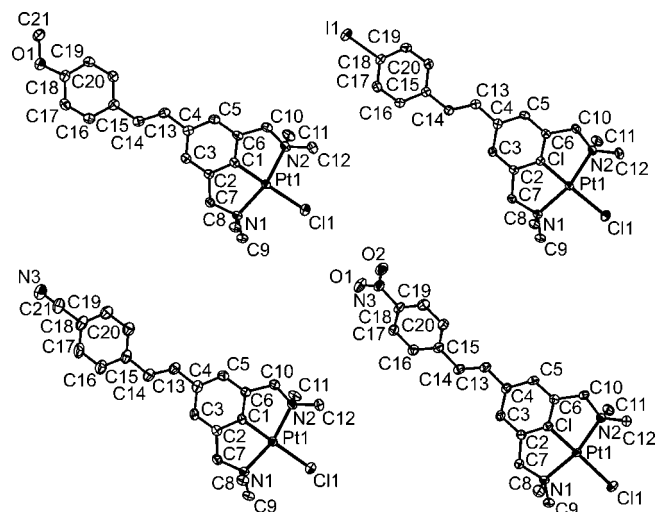


Figure 2. Displacement ellipsoid plot (50% probability level) of complexes **2** (top left), **5** (top right), **6** (bottom left) and **7** (bottom right). Hydrogen atoms have been omitted for clarity.

Compound **1** crystallizes with three independent molecules in the asymmetric unit of which one is disordered about the central double bond (Figure 1). This type of disorder is rather common in *trans*-stilbene and *trans*-azobenzene derivatives.^[45] The two ordered molecules have very similar bond lengths and angles (Table 1) but differ in the conformation of the 4-dimethylaminostyryl fragment (Figure S1, Supporting Information). The overall shape of the molecules is bent; the *C*_{ipso} carbon atoms are 0.448(4) and 0.270(4) Å (for residues 1 and 2, respectively), beneath the least-squares plane of the central double bond (C4–C13–C14–C15). For the corresponding *para* carbon atoms C18, the distances are 0.099(4) and 0.311(4) Å for residues 1 and 2, respectively. In the crystal, the molecules of the metal complex are stacked on top of each other in an antiparallel fashion. These stacks run in the crystallographic [1,0,1] direction (Figure 1). Intermolecular π -stacking interactions could not be observed in this crystal structure.

Despite the different *para* substituents, compounds **2**, **5** and **6** are isostructural in the solid state. They have similar bond lengths and bond angles (Table 2) and also nearly identical conformations and crystal packings. Small differences are observed for intermolecular interactions involving the *para* substituents. Molecular plots of **2**, **5** and **6** are displayed in Figure 2; likewise in the crystal structure of **1**, the molecules have an overall bent shape (Figure 3). Again, the C1 *C*_{ipso} atom and the C18 aryl carbon atom are beneath the plane of the central double bond with values of 0.382(2), 0.363(3) and 0.343(3) for C1 and 0.307(3), 0.307(4) and 0.101(4) for C18. Also, the crystal structures of **2**, **5** and **6** do not express intermolecular π -stacking interactions. There are only weak intermolecular C–H \cdots π and C–H \cdots Cl interactions, and in some crystals C–H \cdots O (compound **2**) and C–H \cdots N (compound **6**) hydrogen bonds are present. The latter certainly do not determine the packing mode because hydrogen bond interactions in **5** are missing.

All molecules are arranged in the crystallographic *b*-direction in an approximately perpendicular orientation with respect to each other (Figure 4). In the crystallographic *a* direction, layers of polar Pt–Cl units alternate with hydrophobic organic layers.

The molecular geometry of **7** in the crystal is very similar to that of compounds **1**, **2**, **5** and **6** (Table 2). The nitro group in the *para* position is slightly rotated out of the plane with an O2–N3–C18–C17 torsion angle of 165.4(3)°. There is also a slight rotation of the *para* nitrophenyl moiety with respect to the central double bond, expressed in a C13–C14–C15–C16 torsion angle of 167.8(3)°. In contrast to compounds **1**, **2**, **5** and **6**, the shape of **7** is not bent; the C1 *C*_{ipso} atom and the C18 phenyl carbon are essentially in

Table 1. Selected bond lengths [Å], angles [°] and torsion angles [°] of [PtCl{NCN(C₂H₂C₆H₄NMe₂-4')-4}] (**1**).

Residue 1		Residue 2		Residue 3 ^[a]	
Pt1–C11	1.918(4)	Pt2–C21	1.934(4)	Pt3–C31	1.915(4)
Pt1–N11	2.094(3)	Pt2–N21	2.084(3)	Pt3–N31	2.085(3)
Pt1–N12	2.088(4)	Pt2–N22	2.088(3)	Pt3–N32	2.090(4)
Pt1–Cl1	2.4129(13)	Pt2–Cl2	2.4152(11)	Pt3–Cl3	2.4134(12)
C113–C114	1.337(6)	C213–C214	1.344(6)	C13A–C14A	1.339(7)
C11–Pt1–N11	82.28(16)	C21–Pt2–N21	82.15(15)	C31–Pt3–N31	82.59(17)
C11–Pt1–N12	81.89(17)	C21–Pt2–N22	82.32(16)	C31–Pt3–N32	82.58(18)
C11–Pt1–Cl1	179.52(12)	C21–Pt2–Cl2	178.12(13)	C31–Pt3–Cl3	175.11(11)
C118–N13–C121	119.1(4)	C218–N23–C221	120.5(4)	C318–N33–C321	121.1(4)
C118–N13–C122	120.8(4)	C218–N23–C222	119.6(4)	C318–N33–C322	121.4(4)
C14–C113–C114–C115	172.1(4)	C24–C213–C214–C215	172.9(4)	C4A–C13A–C14A–C315	172.0(5)
C113–C114–C115–C116	169.6(4)	C213–C214–C215–C216	177.0(4)	C13A–C14A–C315–C316	–175.5(5)
C117–C118–N13–C121	1.4(7)	C217–C218–N23–C221	–23.5(7)	C317–C318–N33–C321	–0.6(6)
Pt1–N11–C17–C12	–29.2(4)	Pt2–N21–C27–C22	29.2(4)	Pt3–N31–C37–C32	–25.8(5)
Pt1–N12–C110–C16	–29.4(4)	Pt2–N22–C210–C26	25.4(4)	Pt3–N32–C310–C36	–29.5(5)
Angle between planes [°]					
[C11–C12–C13–C14–C15–C16], [C115–C116–C117–C118–C119–C120]	14.5(2)	[C21–C22–C23–C24–C25–C26], [C215–C216–C217–C218–C219–C220]	25.5(2)	[C31–C32–C3A–C4A–C5A–C36], [C315–C316–C317–C318–C319–C320]	13.3(2)

[a] Only the major conformation (81% occupancy) of disordered residue 3 is given. As a result of the disorder, the geometrical values are less reliable than for residues 1 and 2.

Table 2. Selected bond lengths [Å], angles [°] and torsion angles [°] of **2**, **5**, **6** and **7**.

	2 (R' = OMe)	5 (R' = I)	6 (R' = CN)	7 (R' = NO ₂)
Pt–C1	1.920(2)	1.917(4)	1.925(3)	1.915(3)
Pt–N1	2.0850(18)	2.087(3)	2.081(2)	2.079(2)
Pt–N2	2.0875(19)	2.091(3)	2.091(2)	2.087(2)
Pt–Cl1	2.4122(6)	2.4130(9)	2.4119(8)	2.4061(7)
C13–C14	1.337(4)	1.345(5)	1.334(5)	1.332(4)
C1–Pt1–N1	81.89(8)	82.01(12)	81.99(11)	82.46(11)
C1–Pt1–N2	82.01(8)	81.87(12)	81.83(11)	82.30(11)
C1–Pt1–Cl1	173.69(6)	173.07(9)	173.47(9)	178.33(9)
Pt1–N1–C7–C2	–32.4(2)	–32.4(3)	–32.2(3)	–28.2(3)
Pt1–N2–C10–C6	–28.5(2)	–28.8(3)	–31.2(3)	–29.0(3)
C4–C13–C14–C15	–171.8(2)	–171.8(3)	–175.4(3)	176.2(3)
C13–C14–C15–C16	177.4(3)	–177.4(4)	174.1(4)	167.8(3)
C21–O1–C18–C17	177.2(2)	–	–	–
C16–C17–C18–I	–	179.0(3)	–	–
C21–C18–C19–C20	–	–	178.1(3)	–
O2–N3–C18–C17	–	–	–	165.4(3)
Angle between planes [C1–C2–C3–C4–C5–C6] and [C15–C16–C17–C18–C19–C20] [°]				
	13.64(12)	21.58(16)	9.06(17)	24.65(14)

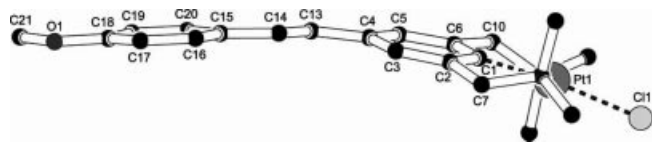


Figure 3. Side view of **2** in the crystal, which shows the overall bent shape. Hydrogen atoms are omitted for clarity. The molecules of **5** and **6** are similarly bent.

the plane of the central double bond (Figure 5). The packing of **7** in the crystal is an antiparallel arrangement in the crystallographic [1,1,0] direction (Figure 6). In the crystallographic *c* direction, polar and apolar layers alternate.

Comparison of the molecular structures of **1**, **2** and **5–7** with earlier reported [PtCl(NCN)] complexes^[21,46–49] shows a similar distorted square-planar geometry around the Pt

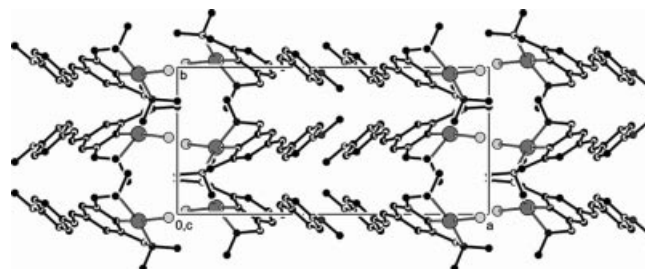


Figure 4. Packing of the molecules in the crystal structure of **2**. Projection along the crystallographic *c* axis. Hydrogen atoms are omitted for clarity. The crystal structures of **5** and **6** are isostructural with **2**.

nucleus in which the carbon atoms of the benzylic substituents (C7 and C10) are positioned above and below the plane

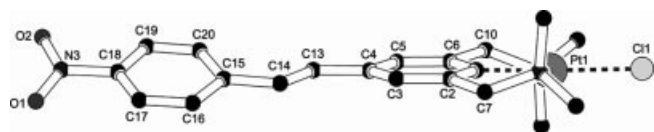


Figure 5. Side view of **7** in the crystal that shows the extended overall shape. Hydrogen atoms are omitted for clarity.

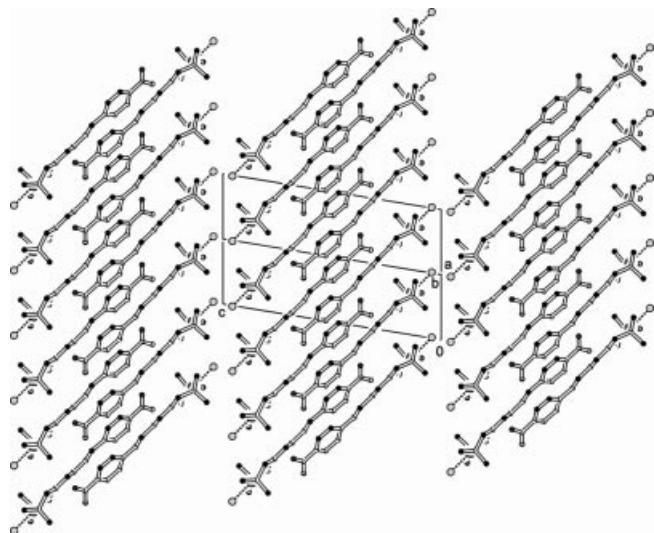


Figure 6. Packing of **7** in the crystal. Hydrogen atoms are omitted for clarity. Projection along the crystallographic $[1, -1, 0]$ direction.

defined by C1–N1–Pt1–N2–C11. For the two five-membered metallacycles, which are slightly puckered, torsion angles for the Pt1–N1–C7–C2 and Pt1–N2–C10–C6 bonds ranging from 25 to 32° were found. The platinum to C_{ipso} (Pt–C) distances of **1**, **2** and **5–7** are in the range of 1.915 to 1.934 Å, as expected.^[47]

For the stilbenoid backbone of **1**, **2** and **5–7**, similar geometric features were found compared to other reported transition-metal-containing stilbenoid fragments.^[9,50,51]

A comparison of the torsion angles between the *trans* bonded 4-styrenyl grouping and the aromatic NCN ring show these fragments to be slightly rotated about the olefinic C–C double bond with torsion angles ranging from 171.8 to 176.2°. For **1** (residues 1 and 3), **2** and **6**, torsion angles between the two aromatic planes (as defined in Tables 1 and 2) of about 9–15° were found. Notable larger torsion angles (ranging from 21° to 26°) were found in **7**, **1** (residue 2) and **5**. As a result of the resonance stabilization energy in conjugated systems, it is expected for stilbenes that the phenyl rings and the ethylene bridge have a nearly coplanar geometry.^[52–55] In practice, torsion angles around 0–5° are commonly found in the solid-state structures,^[56–58] although a small part of the reported stilbenoid molecules show larger torsion angles ranging from 20 to 27°.^[59–61] Such deviations from coplanarity can be explained by a combination of alkenyl–H–*ortho*-H repulsion and by crystal packing forces.

A smaller deviation (1.0–2.7°) from the planar geometry is found for the dihedral angles between the planes formed by the *para* R' substituent (connected to C18) and its ar-

omatic ring (defined by C15–C16–C17–C18–C19–C20), except for **7** (R' = NO₂), of which the nitro group deviates almost 15° from coplanarity (Table 2, Figure 5). This deviation is commonly found for an aromatic nitro group.^[62]

The alternation of bond length δr in the phenyl rings provides information about the presence of possible quinoid character in these rings, which reflects ground-state charge-transfer character.^[63,64] In benzene, the δr value equals 0, whereas values between 0.08 and 0.10 are found in a fully quinoid ring. In the analyses of **2**, **5**, **6** and **7**, for the R'-substituted phenyl ring, δr values between 0.003 and 0.016 are found;^[65] for the metal-substituted ring, values of δr range from 0.015 to 0.019. This indicates that in both substituted rings a slight degree of quinoid character is present. This supports the idea that the metal-containing group acts as an electroactive substituent. The electron donating NMe₂ substituent present in **1**, however, seems to induce more quinoid character in the R' phenyl ring because a value of $\delta r = 0.025$ in residue 1 and 2 is found. The larger contribution into the quinoid character induced by the NMe₂ group was also reported by others.^[66] The effect of the NMe₂ group seems to oppose that of the metal substituent in **1** because a smaller alternation in the bond length ($\delta r = 0.009$ and 0.013 for residue 1 and 2, respectively) occurs here relative to that of **2**, **5**, **6** and **7**.

NMR Spectroscopy

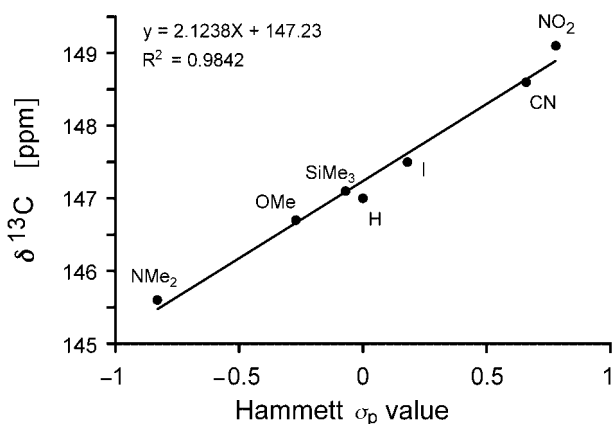
Solutions of **1–7** in CD₂Cl₂ (0.01 M) were studied by ¹H, ¹³C{¹H} and ¹⁹⁵Pt{¹H} NMR spectroscopy. In the ¹H NMR spectra, resonances for the (CH₃)₂N and the ArCH₂N protons of the CH₂NMe₂ substituents were observed at $\delta = 3.04$ –3.05 ppm and at $\delta = 4.02$ –4.08 ppm, respectively, and showed characteristic satellites resulting from platinum coupling [³J(H,Pt) \approx 37 and 46 Hz, respectively]. For compounds **1**, **2** and **4–7**, characteristic resonances of the vinylic protons were observed at $\delta = 6.8$ –7.2 ppm with large coupling constants [³J(H,H) = 16 Hz] indicative of a *trans* configuration. For **3**, the chemical shift difference between the vinylic protons was so small that the coupling was not resolved in the higher order pattern.

In the ¹³C{¹H} NMR spectra of some of the compounds, a two [²J(C,Pt) = 62–67 Hz] or three bond coupling [³J(C,Pt) = 35–37 Hz] of platinum to carbon was observed. A linear correlation was found ($R^2 = 0.9842$) when the ¹³C{¹H} NMR chemical shift of the C_{ipso} (to platinum; Table 3) of **1–7** was plotted against the Hammett σ_p parameter of the *para* R' substituents (Figure 7), which suggests that the effect on the electronic character of the conjugated molecule induced by the different *para* substituents can be experienced within the complete system. A previous correlation study on *para*-substituted stilbenoid ferrocene analogues showed a similar substituent effect^[67] when the ¹³C{¹H} NMR chemical shift of the ferrocenyl carbons was plotted against the Hammett σ_p parameter.

Table 3. NMR spectroscopic data of [PtCl{NCN(C₂H₂C₆H₄-R'-4')-4}] (1–7).^[a]

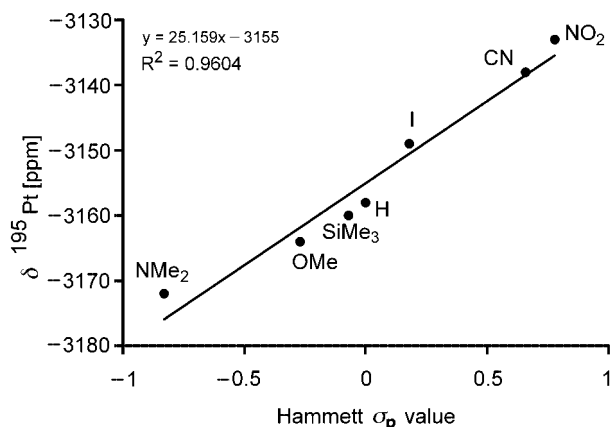
Compound	σ_p Hammett ^[b]	$\delta = {}^{13}\text{C}\{^1\text{H}\}$ [ppm] ^[c]	$\delta = {}^{195}\text{Pt}\{^1\text{H}\}$ [ppm] ^[d]
1 (R = NMe ₂)	-0.83	145.6	-3173
2 (R = OMe)	-0.27	146.7	-3164
3 (R = SiMe ₃)	-0.07	147.1	-3160
4 (R = H)	0.00	147.0	-3158
5 (R = I)	0.18	147.5	-3149
6 (R = CN)	0.66	148.6	-3138
7 (R = NO ₂)	0.78	149.1	-3133

[a] 0.01 M solution in CD₂Cl₂. [b] Obtained from Ref.^[25] [c] Chemical shift of C_{ipso} to Pt. [d] Na₂PtCl₆ as external reference.

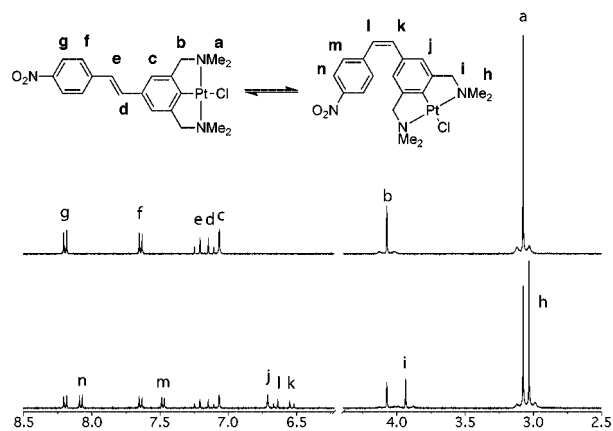
Figure 7. Hammett correlation of the ¹³C{¹H} C_{ipso} NMR chemical shift of 1–7.

The electron density at the metal centre of complexes 1–7 was probed with ¹⁹⁵Pt{¹H} NMR spectroscopy. The sensitivity of the ¹⁹⁵Pt nucleus towards changes in, for instance, the geometry and the oxidation state of the metal centre or changes in the electronic nature of the surrounding ligands, is reflected in the ¹⁹⁵Pt{¹H} NMR chemical shift.^[68] For 1–7, that is, upon going through the series from an electron-donating (NMe₂) to an electron-accepting (NO₂) *para* substituent, the ¹⁹⁵Pt{¹H} NMR chemical shift moves to a higher frequency, which points to a less-shielded platinum nucleus (Table 3). A plot of the ¹⁹⁵Pt{¹H} NMR chemical shift against the Hammett σ_p parameter resulted in a good linear correlation ($R^2 = 0.9604$, Figure 8). The results show the power of the ¹⁹⁵Pt{¹H} NMR chemical shift as a qualitative probe for the electronic character of the molecule (including C_{ipso}) to which the metal is connected. The slope of the line provides information about the efficiency of communication between the substituent and the metal centre, and therefore, it was compared with the slope of a similar graph from an earlier study in which the ¹⁹⁵Pt{¹H} NMR shift of *para*-functionalized phenyl pincers [PtCl(NCN-R-4)] was correlated with the Hammett σ_p parameter.^[23] Indeed, the slope of 25 in the present study found for the stilbenoid NCN-pincer platinum compounds is less steep relative to the 171 found for the [PtCl(NCN-R-4)] compounds earlier. This smaller number is in agreement with

the larger size of the π system in 1–7, over which the effect of the 4-R' group to the 4-PtCl grouping is spread out.

Figure 8. Hammett correlation of the ¹⁹⁵Pt{¹H} NMR chemical shift of 1–7.

As pointed out above, the compounds in solution do undergo *trans*–*cis* isomerization when exposed to light.^[6] Irradiation of a CD₂Cl₂ solution of 7 (9.5×10^{-3} M, $\lambda_{ex} = 365$ nm) for 2 h resulted in a *trans*–*cis* mixture. After 1 h, the photostationary state of the isomerization reaction was reached, and a *trans*–*cis* ratio of exactly 1:1 was observed. In the ¹H NMR spectrum, the formation of the *cis* isomer could be observed by the appearance of new peaks for all the protons (Figure 9). The doublets at $\delta = 6.65$ ppm and $\delta = 6.53$ ppm are assigned to the *cis* protons of the ethylene bridge which have a characteristic *cis* coupling constant, ³ $J(\text{H},\text{H}) = 12$ Hz. Recently, this in-solution *trans*–*cis* isomerization process was also observed by others in a study of cyclometallated Pt^{II} complexes containing substituted 4-styryl-2-phenylpyridine ligands.^[69]

Figure 9. ¹H NMR spectra of 7, before (top; only *trans*) and after (bottom; *trans*–*cis* mixture) UV irradiation (400 MHz, CD₂Cl₂, 9.5×10^{-3} M; $\lambda_{ex} = 365$ nm, 1 h).

UV/Vis Spectroscopy

The complexes are well soluble in dichloromethane, but their solubility decreases in solvents like diethyl ether,

Table 4. UV/Vis maxima (λ_{max}) of [PtCl{NCN(C₂H₂C₆H₄-R'-4')-4}] (1–7).^[a]

Solvent	1 (R = NMe ₂)	2 (R = OMe)	3 (R = SiMe ₃)	4 (R = H)	5 (R = I)	6 (R = CN)	7 (R = NO ₂)
Acetonitrile	366	348	341	347	355	369	402
Dichloromethane	–	244 (10.9)	245 (12.4)	245 (10.8)	249 (8.2)	264 (13.1)	298 (10.7)
	371 (36.9) ^[b]	352 (30.6)	355 (36.0)	350 (35.6)	358 (37.3)	376 (29.4)	413 (20.6)
Tetrahydrofuran	369	353	360	354	363	380	415
Ethyl acetate	367	352	356	351	361	379	413
Diethyl ether	366	352	357	351	361	376	411

[a] Absorption wavelength [nm] at room temperature ($c \approx 10^{-5}$ M), absorption coefficient ϵ [$10^3 \text{ M}^{-1} \text{ cm}^{-1}$] in brackets. [b] Higher energy absorption band not observed.

whereas they are insoluble in cyclohexane. As a result of this restricted solubility, the absorption coefficients of the complexes were only determined in dichloromethane. The absorption spectra for 1–7 (Figure 10, Table 4) show a weak band between 244 and 298 nm (not observed for 1) that originates from the excitation of the singlet ground state (S_0) to a higher excited state (e.g. $S_0 \rightarrow S_2$).^[1] A more intense lower energy band ($S_0 \rightarrow S_1$) is observed in the range of 341 to 415 nm. The position of this band shifts to lower energy with increasing acceptor strength, that is by going from 4 ($R' = \text{H}$) to 7 ($R' = \text{NO}_2$). Therefore, in the presence of an acceptor functionality, this transition involves intramolecular charge transfer (ICT) in which the NCN–PtCl fragment, as anticipated, behaves as a donor functionality. The observed bathochromic shift is in agreement with calculated charge-transfer properties of 4,4'-substituted donor–acceptor stilbenes,^[70] where an increase in the donor–acceptor strength causes the HOMO–LUMO distance of the molecule to decrease, which results in an absorption at lower wavelength. A change in the donor properties of R' by going through the series from 4 to 1 only slightly affects the absorption maximum (λ_{max}) of the compounds.

For comparison of 1–7 with organic 4,4'-substituted donor–acceptor stilbene analogues, DANS was used as a reference system. In Figure 10 it can be seen that the absorption maxima of 7 and DANS are slightly shifted with respect to each other, which reflects the different nature of the PtCl grouping versus the NMe₂ group. Moreover, the absorption measurements of complexes 1–7 in different solvents showed no distinct solvent polarity dependence (Table 4), as was reported previously for the organic stilbene analogues,^[71,72] which points to a nonpolar ground state of the stilbenoid NCN–Pt compounds.

A qualitative screening of the luminescence of solutions of 1–7 in dichloromethane by use of a standard laboratory UV-lamp ($\lambda = 365$ nm) revealed that, surprisingly, both the 4-donor–4'-donor complex 1 and complexes 6 and 7 with a strong donor–acceptor combination are luminescent. Therefore, these complexes were further studied for their photophysical properties by determination of the fluorescence maxima (λ_{fl}), quantum yields (Φ_{fl}) and excited state lifetimes (τ_{fl}). From this data, the radiative (k_{r}) and nonradiative (k_{nr}) decay constants were calculated. Complexes 2–4 showed no luminescence, and complex 5 showed only very weak luminescence, which was too weak to be studied in more detail.

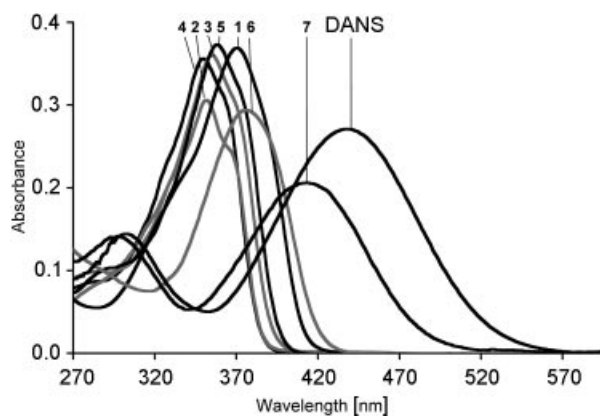


Figure 10. UV/Vis spectra of 1–7 in CH₂Cl₂. Most intense band, from left to right: $R' = \text{H}$ (4), OMe (2), SiMe₃ (3), I (5), NMe₂ (1), CN (6), NO₂ (7) and DANS.

For complexes 1, 6 and 7, the emission spectra and excited state lifetimes were recorded in solvents of different polarity (Tables 5 and 6). For all compounds, a bathochromic shift in the emission maximum with an increase in solvent polarity was observed, as is displayed for 6 in Figure 11. The occurrence of this positive solvatochromism, which is the most extensive for 7, reflects the formation of a charge-separated or dipolar-excited state.

Table 5. Fluorescence data of 1.

Solvent	[PtCl{NCN(C ₂ H ₂ C ₆ H ₄ -NMe ₂ -4')-4}] (1)				
	λ_{fl} [nm] ^[a]	Φ_{fl}	τ_{fl} [ps] ^[b]	k_{r} [$\cdot 10^7 \text{ s}^{-1}$]	k_{nr} [$\cdot 10^9 \text{ s}^{-1}$]
Acetonitrile	454	0.017	289	5.9	3.4
Dichloromethane	432	0.006	307	2.0	3.2
Tetrahydrofuran	429	0.003	537	0.6	1.9
Ethyl acetate	427	0.002	463	0.4	2.2
Diethyl ether	425	0.002	^[c]		

[a] Excitation wavelength 370 nm, argon flushed solutions at room temperature, $c \approx 10^{-6}$ M. [b] Only the values for the slowest component of the biexponential decay curve are reported as the fast component showed values below the detection limit of the setup that was used (<47 ps). [c] Solubility too low to allow measurements.

When the Stokes shift $\nu_{\text{abs}} - \nu_{\text{fl}}$ is plotted versus the solvent polarity parameter Δf (defined by the solvent dielectric constant ϵ and the refractive index n ^[73]) the difference between the ground and excited state dipole moments $\Delta\mu$ for

Table 6. Fluorescence data of **6** and **7**.

Solvent	[PtCl{NCN(C ₂ H ₂ C ₆ H ₄ -CN-4')-4}] (6)					[PtCl{NCN(C ₂ H ₂ C ₆ H ₄ -NO ₂ -4')-4}] (7)				
	$\lambda_{fl}^{[a]}$ [nm]	Φ_{fl}	τ_{fl} [ps]	k_r [$\cdot 10^8$ s ⁻¹]	k_{nr} [$\cdot 10^9$ s ⁻¹]	$\lambda_{fl}^{[a]}$ [nm]	Φ_{fl}	τ_{fl} [ps]	k_r [$\cdot 10^8$ s ⁻¹]	k_{nr} [$\cdot 10^9$ s ⁻¹]
Acetonitrile	476	0.065	271	2.4	3.5	628	0.043	343	1.3	2.8
Dichloromethane	466	0.088	206	4.3	4.4	677	0.018	134	1.3	7.3
Tetrahydrofuran	464	0.080	174	4.6	5.3	592	0.042	278	1.5	3.5
Ethyl acetate	458	0.067	137	4.9	6.8	591	0.068	291	2.3	3.2
Diethyl ether	443	0.023	61	3.8	16.0	546	0.197	573	3.4	1.4

[a] Excitation wavelength 370 nm, argon flushed solutions at room temperature, $c \approx \cdot 10^{-6}$ M.

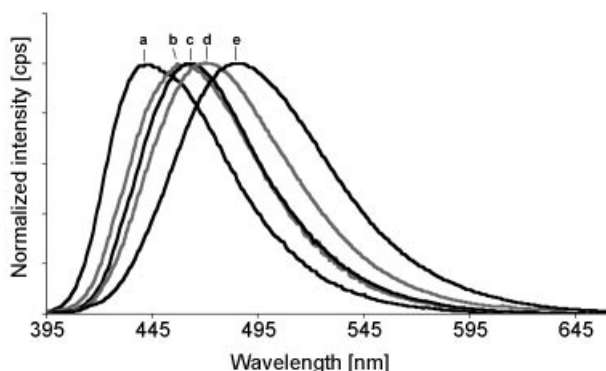


Figure 11. Normalized emission spectra of **6** in different solvents; they show a bathochromic shift with an increase in solvent polarity. Polarity increases from left to right; diethyl ether (a), ethyl acetate (b), tetrahydrofuran (c), dichloromethane (d) and acetonitrile (e).

donor–acceptor systems can be approximated by using the Lippert equation [Equation (1)]^[74]

$$v_{\text{abs}} - v_{\text{fl}} = \frac{2\Delta\mu^2}{hc\rho^3} \Delta f + \text{constant}$$

$$\Delta f = \frac{\epsilon - 1}{2\epsilon + 1} - \frac{n^2 - 1}{2n^2 + 1} \quad (1)$$

where h is Planck's constant and c is the speed of light. The ρ (Onsager cavity radius) of the molecule can be estimated by numerous methods,^[75,76] and in this study the radii of molecules **6** and **7** were estimated from their solid-state structures (estimated to be 4.36 and 4.39 Å, respectively).^[77,78]

From the slopes derived from the Lippert plot of **6** and **7** (the values in dichloromethane were excluded from the trend line, Figure 12), $\Delta\mu$ was estimated to be 11 and 13 D, respectively. This implies that in these systems, excited state charge separation is present but to a lesser extent than that found for related 4,4'-substituted stilbenes.^[79] The larger dipole moment found for **7** is a result of the stronger electron accepting nitro group.

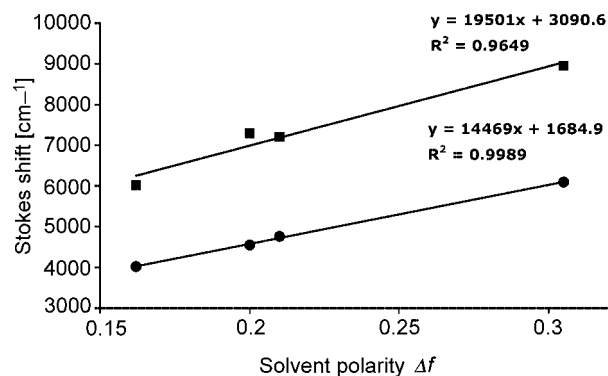
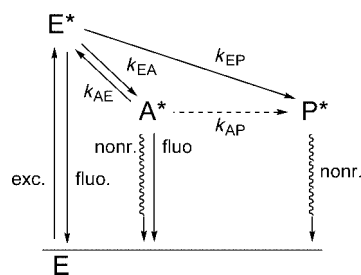


Figure 12. Lippert plot of the Stokes shift versus the solvent polarity parameter Δf for **6** (dots) and **7** (squares).

The excited state behaviour of 4,4'-substituted organic stilbenes has been studied intensively.^[8,80–86] For the excited state of the molecule, a three-state kinetic scheme is suggested (Scheme 4).^[86] The ground state molecule (E) can be excited into the emissive state E* (planar geometry) in which the molecule is suggested to have biradicaloid character. Emission relaxation to the ground state from E* is accompanied by two competing relaxation pathways. One proceeds through the nonemissive “phantom-singlet state” (P*), in which the molecule assumes a twisted conformation (double bond twist, including the *trans-cis* isomerization process),^[6] also referred to as the photochemical funnel toward the ground state. The alternative follows a pathway which involves rotation about a bond between the aromatic moiety and the central double bond and ends up in a twisted intramolecular charge transfer state A* (TICT state), which is considered to be responsible for the main



Scheme 4. The three-state kinetic scheme proposed for the relaxation of 4,4'-substituted organic stilbenes after excitation.

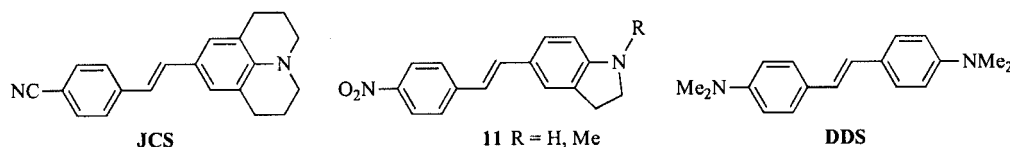


Figure 13. Donor–acceptor stilbenes **JCS** and **11**, donor–donor stilbene **DDS**.

part of the emission. The photophysics of the molecule are dependent on the relative energy of the three different energy states, which are influenced by the solvent polarity and by the donor–acceptor strength of the substituents.

For 4,4'-substituted organic stilbenes in which the donor substituent is an alkylamino group, the TICT state can be reached by a single bond twist about the single bond between the alkylamino group and the aromatic ring or by a twist about the single bond between the anilino group and the double bond. To exclude the alkylamino TICT state, other groups developed and studied the more rigid amino substituted donor–acceptor stilbenes **JCS**^[84] and **11**^[72] (Figure 13). In our study, the excited state behaviour of **6** and **7** will be compared with that of **JCS** and **11**, respectively, with regard to the NCN–PtCl fragment of **6** and **7** as the rigid donor fragment. So far, we were not able to find a rigid reference system for **1** in the literature; therefore, it was compared with **DDS**^[82] (Figure 13), which contains two NMe₂ groups.

The fluorescence quantum yields of **1** range from 0.002 to 0.017, and they are remarkably low relative to the values found for **DDS** (ranging from 0.39 to 0.57). Presumably, the presence of the NCN–PtCl fragment favours nonradiative decay by accelerating intersystem crossing. The fluorescence quantum yields of **1** slightly increase with increasing solvent polarity (Table 5), which is probably due to stabilization of the A* state with increasing solvent polarity.^[82,87] The fluorescence lifetimes of **1** at room temperature, which were derived from a biexponential decay curve (Table 5; only the slower components of the decay curves are reported here, ranging from 289 to 537 ps), decrease with increasing solvent polarity and are shorter than the value found for **DDS** (900 ps in ethanol at 300 K). It must be noted that the nonradiative decay rates [$k_{nr} = (1 - \Phi_f)/\tau_f$] increase with increasing solvent polarity. In more polar solvents, the low-lying A* state is increasingly populated, and the smaller energetic distance to the ground state favours nonradiative decay.

For **6**, an increase in the quantum yield and the lifetime is observed when the polarity of the solvent increases, which can be explained by the dipolar character of the states involved. Both E* and A* are highly polar, with an increased dipole moment for A*; P* has weak or nonpolar properties.^[83] Therefore, an increase in the solvent polarity stabilizes E* and A*, and to a much lesser extent P*. As a result, the nonradiative decay, which is governed by the access to P*, becomes less important. For **6**, indeed a decrease in k_{nr} with increasing solvent polarity is found. This is in agreement with what was found for **JCS**,^[83,84] for which the yield of the nonradiative decay also decreases with increasing solvent polarity.

For **7**, a reverse dependency of the fluorescence lifetime and quantum yield on the solvent polarity was found. Roughly, an increase in the fluorescence quantum yield and the fluorescence lifetime was observed when the solvent polarity decreases. The remarkable change in the photophysical properties accompanying the change of a cyano group to a nitro group was studied intensively,^[72] and the change is also found for **11**. As a consequence of its larger dipole moment, an increase in the solvent polarity results in a decreased energy level of the A* state of **7**. The lower energy minimizes the distance from A* to the ground state and causes radiationless decay from A* to compete with fluorescence. As a result from the energetically low-lying A* state, the P* level plays no significant role, and therefore, relaxation proceeds primarily by way of the A* state.

Conclusions

A useful and efficient synthetic route towards electronically tunable organometallic stilbenes based on a series of stilbenoid NCN–Pt^{II} pincers is reported. The *trans* configuration of the complexes is maintained in the solid state, but in solution they undergo *trans*–*cis* isomerization upon exposure to light. The physical data reported for compounds **1**–**7** reflect that a substituent effect can be experienced within the complete delocalized π -system. The linear correlation found between the ¹³C{¹H} and ¹⁹⁵Pt{¹H} NMR chemical shifts and the Hammett σ_p value indicates that the metal is sensitive to the change in the electronic properties of the delocalized π -system. In this way the metal centre can communicate with a substituent that is situated quite a distance from itself. Therefore, we can regard the platinum centre as a probe by using the ¹⁹⁵Pt{¹H} NMR chemical shift data as a readout for the electronic properties of a conjugated system that is connected to it. The UV/Vis and fluorescence study show that the NCN–PtCl fragment can be qualitatively regarded as an electron-donating group. From the low quantum yields and fast decay rates, it can be concluded that the presence of the platinum centre favours nonradiative decay when compared with the organic stilbene analogues.

Experimental Section

General: All reactions involving air- or moisture-sensitive reagents were performed by using standard Schlenk techniques unless stated otherwise. Light-sensitive compounds and solutions were protected from the light with the use of aluminium foil. Pentane, THF and Et₂O were distilled from Na/benzophenone, CH₂Cl₂ was distilled

from CaH₂ and triethylamine was distilled from KOH prior to use. The platinum precursor [Pt(*p*-tol)₂(SEt₂)₂]^[88,89] [PtBr(NCN-CHO-4)]^[90] trimethyl(*p*-tolyl)silane^[91] and the respective *para*-substituted diethyl benzylphosphonates **8b–g** were prepared according to published procedures of which the benzylic bromination step was performed according to the published procedure of Amijs and coworkers.^[39] All other reagents were commercially available and used without further purification. ¹H and ¹³C{¹H} NMR spectra were recorded at 25 °C with a Bruker AC 300 NMR or Varian Inova 300 or Varian 400 spectrometers, chemical shifts are reported relative to residual solvent resonances. ¹⁹⁵Pt{¹H} NMR spectra were recorded with a Varian Inova 300 MHz NMR spectrometer, referenced to external Na₂PtCl₆ (1 M in D₂O, δ = 0 ppm).^[92] Elemental analyses were performed by Kolbe, Mikroanalytisches Laboratorium (Mülheim a.d. Ruhr, Germany). ES-MS spectra were obtained from the Biomolecular Mass Spectrometry Group at the Utrecht University. Infrared spectra were recorded with a Perkin–Elmer Spectrum 1 FTIR spectrometer. UV spectra were collected with Cary 1 or Cary 5 spectrophotometers in spectrophotometric-grade solvents. Fluorescence emission spectra were obtained with a Spex Fluorolog instrument, equipped with a Spex 1680 double excitation monochromator, a Spex 1681 emission monochromator and a Spex 1911F detector. Fluorescence spectra were corrected for the detector spectral response with the aid of a correction file provided by the manufacturer. Fluorescence quantum yields were determined relative to 9,10-diphenylanthracene (Φ_f = 0.90, excitation wavelength 370 nm).^[93] Solvents used for fluorescence measurements were of spectrophotometric grade (Acros). Lifetime measurements were performed with the use of a Pico Quant PDL 800-B laser as the excitation source (λ_{exc} = 406 nm, 55 ps pulse width, 2.5–40 MHz repetition rate). The luminescence was collected through a focusing lens, filtered through a crossed polarizer and a combination of suitable optical cut-off filters, dispersed by a 0.1 m monochromator (1350 lines mm⁻¹ grating, blazed at 500 nm) and detected by a fast Hamamatsu photomultiplier tube (PMT) (H5738P-01). The PMT signal was amplified by an inverting preamplifier (PAM-102-T – PicoQuant) and used as the start input for a Time Harp 200 multichannel computer card, which was synchronized with the laser pulse by the stop input. The decay curves were obtained by time-correlated single photon counting (TCSPC) by time-to-amplitude conversion (TAC). The ratio of stop to start pulses was kept low (below 0.04) to assure good statistics. The instrument response function (IRF) was measured by using a dilute suspension of silica particles (LUDOX) as the scattering medium and the same experimental conditions used for the fluorescence decay measurements. The raw data was deconvoluted from the IRF and analyzed by fluorescence decay analysis software (Fluofit 3.3). The instrumental resolution was 30 ps (10% of the IRF FWHM).

Diethyl 4-Dimethylaminobenzylphosphonate (8a): At 0 °C, methanesulfonyl chloride (0.54 mL, 6.98 mmol) was added dropwise to a solution of 4-dimethylaminobenzyl alcohol (1.0 g, 6.61 mmol) and triethylamine (1.12 mL) in dichloromethane (20 mL). After complete addition, the solution was warmed to room temperature for 1 h. Next, all volatiles were evaporated, and triethylphosphite (4 mL) and NaI (400 mg, 2.67 mmol) were added to the oily residue. The mixture was heated at 110 °C for 2.5 h after which the excess triethylphosphite was distilled off in vacuo. At room temperature, water (10 mL) and ethyl acetate (20 mL) were subsequently added to the residue. The organic layer was separated, washed with saturated NaHCO₃ (5 mL) and NaCl solution (5 mL), and dried using Na₂SO₄. After evaporation and Kügelrohr distillation, an oily product (0.9 g) was obtained. Further purification of the product could be achieved by column chromatography [neutral

Al₂O₃, hexane/ethyl acetate (9:1), then gradient elution increasing to pure ethyl acetate] and **8a** (455 mg, 1.68 mmol, 25%) was isolated as an oil. ¹H NMR (300 MHz, C₆D₆): δ = 7.29 [dd, ³J(H,H) = 8.9 Hz, ⁴J(H,H) = 2.5 Hz, 2 H, ArH], 6.57 [d, ³J(H,H) = 8.5 Hz, 2 H, ArH], 3.89 (m, 4 H, OCH₂), 3.02 [d, ²J(H,P) = 20.9 Hz, 2 H, CH₂P], 2.49 [s, 6 H, N(CH₃)₂], 0.97 [t, ³J(H,H) = 7.1 Hz, 6 H, CH₃] ppm. ¹³C{¹H} NMR (75 MHz, C₆D₆): δ = 149.8, 130.8 [d, J(C,P) = 6.5 Hz], 119.7 [d, J(C,P) = 9.3 Hz], 113.0, 61.7 [d, J(C,P) = 6.5 Hz], 40.2, 33.1 [d, J(C,P) = 139.5 Hz, CH₂P], 16.5 [d, J(C,P) = 5.4 Hz] ppm. IR (ATR): ν̄ = 2980, 2906, 2801, 1736, 1615, 1567, 1521, 1479, 1445, 1391, 1348, 1243, 1201, 1191, 1163, 1097, 1052, 1022, 945, 847, 822, 774, 731, 717, 689 cm⁻¹. MS (ES+, CH₂Cl₂): *m/z* = 272.15 [M + H]⁺. C₁₃H₂₂NO₃P (271.30): calcd. C 57.55, H 8.17, N 5.16; found C 57.42, H 8.24, N 5.09.

[PtCl(NCN-CHO-4)] (9): [PtBr(NCN-CHO-4)] (1.19 g, 2.40 mmol) in wet acetone (10 mL) was treated with AgBF₄ (0.49 g, 2.52 mmol) for 1 h, and the formed precipitate was filtered through Celite. To the filtrate, a solution of NaCl (1.4 g, 23 mmol) in demineralized water (2 mL) was added, and the mixture was stirred for 1.5 h after which all the volatiles were removed in vacuo. After the addition of demineralized water (15 mL) and CH₂Cl₂ (15 mL), the mixture was filtered through Celite. The residue was extracted with dichloromethane (3 × 15 mL) after which the organic fraction of the filtrate was separated. The organic fraction was dried with MgSO₄, filtered and concentrated in vacuo to yield the crude product as a solid. Purification by column chromatography (CH₂Cl₂/MeOH, 9:1, SiO₂) yielded **9** (0.86 g, 1.91 mmol, 80%) as a light yellow solid. ¹H NMR (300 MHz, CD₂Cl₂): δ = 9.82 (s, 1 H, CHO), 7.32 (s, 2 H, ArH), 4.08 [s, ³J(H,Pt) = 46.2 Hz, 4 H, CH₂], 3.05 [s, ³J(H,Pt) = 38.2 Hz, 12 H, CH₃] ppm. ¹³C{¹H} NMR (75 MHz, CD₂Cl₂): δ = 192.0 (CHO), 157.5 (C_{ipso} to Pt), 144.7 (C_{ortho} to Pt), 133.4, 121.4 [³J(C,Pt) = 35.6 Hz; C_{meta} to Pt], 77.3 [²J(C,Pt) = 61.0 Hz; NCH₂], 54.5 [N(CH₃)₂] ppm. ¹⁹⁵Pt{¹H} NMR (64 MHz, CD₂Cl₂): δ = -3068 ppm. IR (ATR): ν̄ = 3017, 2980, 2929, 1674 (C=O), 1398, 737 cm⁻¹. MS (ES+, CH₃CN): *m/z* = 455.14 [M - Cl + CH₃CN]⁺, 414.10 [M - Cl]⁺. C₁₃H₁₉ClN₂O₂Pt (449.84): calcd. C 34.71, H 4.26, N 6.23; found C 34.80, H 4.19, N 6.17.

General Procedure for the Preparation of Stilbenoid Pincer Compounds 1–7: In a dry Schlenk tube, *para*-aldehyde substituted pincer platinum derivative **9** and the appropriate phosphonate ester **8** were dissolved in dry degassed THF (10–15 mL). While stirring, *t*BuOK (2.5 equiv.) was added to the reaction mixture, under a nitrogen outflow, which directly caused a strong colour change of the reaction mixture. Upon completion of the reaction, monitored by TLC, the mixture was quenched at 0 °C by the addition of ice and an aqueous NaCl solution (to prevent halogen abstraction on the Pt centre). The formed precipitate was isolated by filtration through a glass filter. The residue was dissolved in dichloromethane, dried with MgSO₄, filtered and evaporated to leave the crude product. The crude product was purified by precipitation out of a small amount of dichloromethane by the addition of pentane.

[PtCl{NCN(C₂H₂C₆H₄-NMe₂-4')-4}] (1): Diethyl 4-dimethylaminobenzylphosphonate (**8a**; 100 mg, 0.369 mmol), **9** (150 mg, 0.334 mmol). Product isolated as a pale yellow powder (171 mg, 0.302 mmol, 90%). ¹H NMR (300 MHz, CD₂Cl₂): δ = 7.37 [d, ³J(H,H) = 8.8 Hz, 2 H, ArH], 6.97 [d, ³J(H,H) = 16.2 Hz, 1 H, *trans* CH=CH], 6.96 (s, 2 H, ArH), 6.81 [d, ³J(H,H) = 16.8 Hz, 1 H, *trans* CH=CH], 6.70 [d, ³J(H,H) = 8.8 Hz, 2 H, ArH], 4.02 [s, ³J(H,Pt) = 46.2 Hz, 4 H, CH₂], 3.04 [s, ³J(H,Pt) = 37.9 Hz, 12 H, CH₃], 2.96 (s, 6 H, CH₃) ppm. ¹³C{¹H} NMR (75 MHz, CD₂Cl₂): δ = 150.4 [ArCN(CH₃)₂], 145.6 (C_{ipso} to Pt), 144.2, 134.0, 127.4, 126.5, 126.2, 125.8, 117.6 [³J(C,Pt) = 34.9 Hz; C_{meta} to Pt], 112.8,

77.9 [$^2J(\text{C},\text{Pt}) = 66.5 \text{ Hz}$; CH_2N], 54.6 [$\text{CH}_2\text{N}(\text{CH}_3)_2$], 40.6 [$\text{ArN}(\text{CH}_3)_2$] ppm. $^{195}\text{Pt}\{^1\text{H}\}$ NMR (64 MHz, CD_2Cl_2): $\delta = -3173$ ppm. IR (ATR): $\tilde{\nu} = 3009, 2978, 2916, 2797, 1604, 1520, 1448, 1351, 1271, 1217, 1187, 1167, 1157, 1127, 1084, 1060, 1041, 944, 880, 835, 808, 706 \text{ cm}^{-1}$. MS (ES+, $\text{CH}_3\text{CN}/\text{CH}_2\text{Cl}_2$): $m/z = 566.17$ [$\text{M}]^+$, 531.19 [$\text{M} - \text{Cl}]^+$. $\text{C}_{22}\text{H}_{30}\text{ClN}_3\text{Pt}$ (566.18): calcd. C 46.60, H 5.33, N 7.41; found C 46.68, H 5.31, N 7.36.

[PtCl₂NCN(C₂H₅C₆H₄-OMe-4')-4] (2): Diethyl 4-methoxybenzylphosphonate (**8b**; 126 mg, 0.488 mmol), **9** (200 mg, 0.445 mmol). Product isolated as a yellow powder (132 mg, 0.238 mmol, 53%). ^1H NMR (300 MHz, CD_2Cl_2): $\delta = 7.43$ [d, $^3J(\text{H},\text{H}) = 8.8 \text{ Hz}$, 2 H, ArH], 7.00 [d, $^3J(\text{H},\text{H}) = 16.2 \text{ Hz}$, 1 H, *trans* CH=CH], 6.97 (s, 2 H, ArH), 6.88 [d, $^3J(\text{H},\text{H}) = 8.8 \text{ Hz}$, 2 H, ArH], 6.87 [d, $^3J(\text{H},\text{H}) = 16.2 \text{ Hz}$, 1 H, *trans* CH=CH], 4.08 [s, $^3J(\text{H},\text{Pt}) = 45.9 \text{ Hz}$, 4 H, CH₂], 3.81 (s, 3 H, OCH₃), 3.05 [s, $^3J(\text{H},\text{Pt}) = 37.0 \text{ Hz}$, 12 H, CH₃] ppm. $^{13}\text{C}\{^1\text{H}\}$ NMR (75 MHz, CD_2Cl_2): $\delta = 159.4$ (ArCOMe), 146.7 (C_{ipso} to Pt), 144.2, 133.4, 131.0, 128.1, 127.5, 125.4, 117.6 [$^2J(\text{C},\text{Pt}) = 36.0 \text{ Hz}$; C_{meta} to Pt], 114.4, 77.9 [$^2J(\text{C},\text{Pt}) = 62.1 \text{ Hz}$; CH_2N], 55.6 (OCH₃), 54.5 [$\text{N}(\text{CH}_3)_2$] ppm. $^{195}\text{Pt}\{^1\text{H}\}$ NMR (64 MHz, CD_2Cl_2): $\delta = -3164$ ppm. IR (ATR): $\tilde{\nu} = 3003, 2973, 2921, 2838, 1625, 1604, 1572, 1509, 1451, 1297, 1252, 1174, 1109, 1083, 1029, 965, 881, 855, 833, 808, 734, 722, 705 \text{ cm}^{-1}$. MS (ES+, CH_3CN): $m/z = 559.19$ [$\text{M} - \text{Cl} + \text{CH}_3\text{CN}]^+$, 518.12 [$\text{M} - \text{Cl}]^+$. $\text{C}_{21}\text{H}_{27}\text{ClN}_2\text{OPt}$ (553.99): calcd. C 45.53, H 4.91, N 5.06; found C 45.46, H 4.87, N 4.88.

[PtCl₂NCN(C₂H₅C₆H₄-SiMe₃-4')-4] (3): Diethyl 4-trimethylsilylbenzylphosphonate (**8c**; 146 mg, 0.486 mmol), **9** (200 mg, 0.445 mmol). Product isolated as a pale white powder (230 mg, 0.386 mmol, 87%). ^1H NMR (300 MHz, CD_2Cl_2): $\delta = 7.50$ [d, $^3J(\text{H},\text{H}) = 8.3 \text{ Hz}$, 2 H, ArH], 7.47 [d, $^3J(\text{H},\text{H}) = 8.3 \text{ Hz}$, 2 H, ArH], 7.05 (s, 2 H, ArH), 7.01 (s, 2 H, CH=CH), 4.04 [s, $^3J(\text{H},\text{Pt}) = 45.7 \text{ Hz}$, 4 H, CH₂], 3.05 [s, $^3J(\text{H},\text{Pt}) = 37.4 \text{ Hz}$, 12 H, CH₃], 0.272 [s, 9 H, Si(CH₃)₃] ppm. $^{13}\text{C}\{^1\text{H}\}$ NMR (75 MHz, CD_2Cl_2): $\delta = 147.1$ (C_{ipso} to Pt), 144.4, 139.8, 138.7, 134.1, 133.1, 130.5, 125.9, 125.7, 118.0 [$^2J(\text{C},\text{Pt}) = 34.9 \text{ Hz}$; C_{meta} to Pt], 77.9 [$^2J(\text{C},\text{Pt}) = 64.3 \text{ Hz}$; CH_2N], 54.6 [$\text{N}(\text{CH}_3)_2$], -1.1 [Si(CH₃)₃] ppm. $^{195}\text{Pt}\{^1\text{H}\}$ NMR (64 MHz, CD_2Cl_2): $\delta = -3160$ ppm. IR (ATR): $\tilde{\nu} = 3013, 2953, 1625, 1581, 1451, 1396, 1335, 1298, 1248, 1111, 1084, 1015, 964, 832, 804, 755, 719, 691, 670 \text{ cm}^{-1}$. MS (ES+, CH_2Cl_2): $m/z = 596.21$ [$\text{M} + \text{H}]^+$, 560.22 [$\text{M} - \text{Cl}]^+$. $\text{C}_{23}\text{H}_{33}\text{ClN}_2\text{PtSi}$ (596.14): calcd. C 46.34, H 5.58, N 4.70; found C 46.28, H 5.64, N 4.73.

[PtCl₂NCN(C₂H₅C₆H₃)-4] (4): Diethyl benzylphosphonate (**8d**; 61 mg, 0.267 mmol), **9** (100 mg, 0.222 mmol). Product isolated as a pale white powder (92 mg, 0.176 mmol, 79%). ^1H NMR (300 MHz, CD_2Cl_2): $\delta = 7.49$ [d, $^3J(\text{H},\text{H}) = 7.1 \text{ Hz}$, 2 H, ArH], 7.33 [t, $^3J(\text{H},\text{H}) = 7.1 \text{ Hz}$, 2 H, ArH], 7.23 [t, $^3J(\text{H},\text{H}) = 7.1 \text{ Hz}$, 1 H, ArH], 7.06 [d, $^3J(\text{H},\text{H}) = 15.9 \text{ Hz}$, 1 H, *trans* CH=CH], 7.01 [d, $^3J(\text{H},\text{H}) = 15.9 \text{ Hz}$, 1 H, *trans* CH=CH], 7.00 (s, 2 H, ArH), 4.04 [s, $^3J(\text{H},\text{Pt}) = 45.9 \text{ Hz}$, 4 H, CH₂], 3.05 [s, $^3J(\text{H},\text{Pt}) = 37.9 \text{ Hz}$, 12 H, CH₃] ppm. $^{13}\text{C}\{^1\text{H}\}$ NMR (75 MHz, CD_2Cl_2): $\delta = 147.0$ (C_{ipso} to Pt), 144.4, 138.3, 133.1, 130.3, 129.0, 127.4, 126.4, 125.8, 117.9 (C_{meta} to Pt), 77.9 (CH_2N), 54.6 [$\text{N}(\text{CH}_3)_2$] ppm. $^{195}\text{Pt}\{^1\text{H}\}$ NMR (64 MHz, CD_2Cl_2): $\delta = -3158$ ppm. IR (ATR): $\tilde{\nu} = 3018, 2973, 2920, 1625, 1581, 1496, 1450, 1334, 1300, 1085, 964, 831, 753, 708, 692 \text{ cm}^{-1}$. MS (ES+, $\text{CH}_3\text{CN}/\text{CH}_2\text{Cl}_2$): $m/z = 529.18$ [$\text{M} - \text{Cl} + \text{CH}_3\text{CN}]^+$, 488.12 [$\text{M} - \text{Cl}]^+$. $\text{C}_{20}\text{H}_{25}\text{ClN}_2\text{Pt}$ (523.96): calcd. C 45.85, H 4.81, N 5.35; found C 45.76, H 4.88, N 5.23.

[PtCl₂NCN(C₂H₅C₆H₄-I-4')-4] (5): Diethyl 4-iodobenzylphosphonate (**8e**; 86 mg, 0.243 mmol), **9** (100 mg, 0.222 mmol). Product isolated as a light yellow powder (123 mg, 0.189 mmol, 85%). ^1H NMR (300 MHz, CD_2Cl_2): $\delta = 7.66$ [d, $^3J(\text{H},\text{H}) = 8.2 \text{ Hz}$, 2 H, ArH], 7.25 [d, $^3J(\text{H},\text{H}) = 8.2 \text{ Hz}$, 2 H, ArH], 7.04 [d, $^3J(\text{H},\text{H}) =$

16.2 Hz, 1 H, *trans* CH=CH], 6.95 [d, $^3J(\text{H},\text{H}) = 16.2 \text{ Hz}$, 1 H, *trans* CH=CH], 6.99 (s, 2 H, ArH), 4.04 [s, $^3J(\text{H},\text{Pt}) = 45.1 \text{ Hz}$, 4 H, CH₂], 3.05 [s, $^3J(\text{H},\text{Pt}) = 37.4 \text{ Hz}$, 12 H, CH₃] ppm. $^{13}\text{C}\{^1\text{H}\}$ NMR (75 MHz, CD_2Cl_2): $\delta = 147.5$ (C_{ipso} to Pt), 144.4, 138.1, 138.0, 132.7, 131.2, 128.2, 124.6, 118.0 (C_{meta} to Pt), 92.1, 77.9 (CH_2N), 54.6 [$\text{N}(\text{CH}_3)_2$] ppm. $^{195}\text{Pt}\{^1\text{H}\}$ NMR (64 MHz, CD_2Cl_2): $\delta = -3149$ ppm. IR (ATR): $\tilde{\nu} = 3002, 2972, 2920, 1622, 1586, 1575, 1483, 1450, 1430, 1398, 1334, 1183, 1085, 1001, 967, 833, 806, 730, 711 \text{ cm}^{-1}$. MS (ES+, $\text{CH}_3\text{CN}/\text{CH}_2\text{Cl}_2$): $m/z = 649.06$ [$\text{M}]^+$, 614.10 [$\text{M} - \text{Cl}]^+$. $\text{C}_{20}\text{H}_{24}\text{ClIN}_2\text{Pt}$ (649.86): calcd. C 36.96, H 3.72, N 4.31; found C 37.04, H 3.78, N 4.28.

[PtCl₂NCN(C₂H₅C₆H₄-CN-4')-4] (6): Diethyl 4-cyanobenzylphosphonate (**8f**; 155 mg, 0.612 mmol), **9** (250 mg, 0.556 mmol). Product isolated as a yellow powder (275 mg, 0.501 mmol, 90%). ^1H NMR (300 MHz, CD_2Cl_2): $\delta = 7.61$ [d, $^3J(\text{H},\text{H}) = 8.5 \text{ Hz}$, 2 H, ArH], 7.39 [d, $^3J(\text{H},\text{H}) = 8.3 \text{ Hz}$, 2 H, ArH], 7.15 [d, $^3J(\text{H},\text{H}) = 16.5 \text{ Hz}$, 1 H, *trans* CH=CH], 7.04 [d, $^3J(\text{H},\text{H}) = 16.5 \text{ Hz}$, 1 H, *trans* CH=CH], 7.02 (s, 2 H, ArH), 4.05 [s, $^3J(\text{H},\text{Pt}) = 45.6 \text{ Hz}$, 4 H, CH₂], 3.05 [s, $^3J(\text{H},\text{Pt}) = 37.7 \text{ Hz}$, 12 H, CH₃] ppm. $^{13}\text{C}\{^1\text{H}\}$ NMR (75 MHz, CD_2Cl_2): $\delta = 148.6$ (C_{ipso} to Pt), 144.5, 142.9, 134.0, 132.8, 132.1, 126.7, 123.8, 119.5 (CN), 118.3 [$^2J(\text{C},\text{Pt}) = 37.1 \text{ Hz}$; C_{meta} to Pt], 110.2, 77.8 [$^2J(\text{C},\text{Pt}) = 64.3 \text{ Hz}$; CH_2N], 54.5 [$\text{N}(\text{CH}_3)_2$] ppm. $^{195}\text{Pt}\{^1\text{H}\}$ NMR (64 MHz, CD_2Cl_2): $\delta = -3138$ ppm. IR (ATR): $\tilde{\nu} = 2972, 2919, 2223$ (CN), 1664, 1626, 1599, 1579, 1505, 1450, 1333, 1172, 1084, 1016, 955, 882, 864, 833, 818, 725, 707 cm^{-1} . MS (ES+, CH_3CN): $m/z = 554.19$ [$\text{M} - \text{Cl} + \text{CH}_3\text{CN}]^+$, 513.16 [$\text{M} - \text{Cl}]^+$. $\text{C}_{21}\text{H}_{24}\text{ClN}_3\text{Pt}$ (548.97): calcd. C 45.95, H 4.41, N 7.65; found C 46.08, H 4.51, N 7.54.

[PtCl₂NCN(C₂H₅C₆H₄-NO₂-4')-4] (7): Diethyl 4-nitrobenzylphosphonate (**8g**; 122 mg, 0.447 mmol), **9** (182 mg, 0.405 mmol). Product isolated as a brown-red powder (166 mg, 0.292 mmol, 72%). ^1H NMR (300 MHz, CD_2Cl_2): $\delta = 8.18$ [d, $^3J(\text{H},\text{H}) = 8.8 \text{ Hz}$, 2 H, ArH], 7.62 [d, $^3J(\text{H},\text{H}) = 8.8 \text{ Hz}$, 2 H, ArH], 7.21 [d, $^3J(\text{H},\text{H}) = 16.4 \text{ Hz}$, 1 H, *trans* CH=CH], 7.10 [d, $^3J(\text{H},\text{H}) = 16.4 \text{ Hz}$, 1 H, *trans* CH=CH], 7.05 (s, 2 H, ArH), 4.06 [s, $^3J(\text{H},\text{Pt}) = 46.7 \text{ Hz}$, 4 H, CH₂], 3.06 [s, $^3J(\text{H},\text{Pt}) = 37.4 \text{ Hz}$, 12 H, CH₃] ppm. $^{13}\text{C}\{^1\text{H}\}$ NMR (75 MHz, CD_2Cl_2): $\delta = 149.1$ (C_{ipso} to Pt), 146.6, 145.1, 144.6, 135.1, 132.0, 126.7, 124.5, 123.4, 118.5 [$^2J(\text{C},\text{Pt}) = 34.9 \text{ Hz}$; C_{meta} to Pt], 77.8 [$^2J(\text{C},\text{Pt}) = 63.2 \text{ Hz}$; CH_2N], 54.6 [$\text{N}(\text{CH}_3)_2$] ppm. $^{195}\text{Pt}\{^1\text{H}\}$ NMR (64 MHz, CD_2Cl_2): $\delta = -3133$ ppm. IR (ATR): $\tilde{\nu} = 2978, 2917, 1624, 1592, 1573, 1506, 1450, 1333, 1312, 1180, 1107, 1086, 1020, 955, 910, 859, 839, 749, 711, 691 \text{ cm}^{-1}$. MS (ES+, CH_3CN): $m/z = 574.15$ [$\text{M} - \text{Cl} + \text{CH}_3\text{CN}]^+$, 533.15 [$\text{M} - \text{Cl}]^+$. $\text{C}_{20}\text{H}_{24}\text{ClN}_3\text{O}_2\text{Pt}$ (568.96): calcd. C 42.22, H 4.25, N 7.39; found C 42.08, H 4.20, N 7.28.

X-ray Crystal Structure Determinations: X-ray intensities were measured with a Nonius KappaCCD diffractometer with rotating anode and graphite monochromator ($\lambda = 0.71073 \text{ \AA}$) at a temperature of 150 K. The structures were solved with automated Patterson methods^[94] and refined with SHELXL-97^[95] against F^2 of all reflections. The initial atomic coordinates of **2** were taken from isostructural compound **6**. Geometry calculations and checking for higher symmetry were performed with the PLATON^[96] program. In structure **1**, the CH_2Cl_2 solvent molecule was refined with a partial occupation. One of the metal complexes was disordered about the central double bond. In **1** and **7**, hydrogen atoms were introduced in geometrically optimized positions and refined with a riding model. In **2**, **5** and **6**, all hydrogen atoms were located in the difference Fourier map and refined with a riding model. Further crystallographic details are given in Table 7. CCDC-626890 (compound **1**), -626891 (compound **2**), -626892 (compound **5**), -626893 (compound **6**) and -626894 (compound **7**) contain the supplement-

Table 7. Details of the crystal structure determinations.

Compound	1	2	5	6	7
Formula	C ₂₂ H ₃₀ ClN ₃ Pt·0.117CH ₂ Cl ₂ C ₂₁ H ₂₇ ClN ₂ OPt		C ₂₀ H ₂₄ ClIN ₂ Pt	C ₂₁ H ₂₄ ClN ₃ Pt	C ₂₀ H ₂₄ ClN ₃ O ₂ Pt
Fw	576.94	553.99	649.85	548.97	568.96
Crystal size [mm ³]	0.20 × 0.05 × 0.01	0.50 × 0.38 × 0.25	0.27 × 0.27 × 0.09	0.18 × 0.18 × 0.06	0.42 × 0.21 × 0.06
Crystal colour	colourless	yellow	colourless	yellow	orange
Crystal system	monoclinic	monoclinic	monoclinic	monoclinic	triclinic
Space group	C2/c (no. 15)	P2 ₁ /c (no. 14)	P2 ₁ /c (no. 14)	P2 ₁ /c (no. 14)	P $\bar{1}$ (no. 2)
a [Å]	46.607(3)	18.7368(2)	18.4773(1)	18.3890(3)	6.1928(1)
b [Å]	8.4291(5)	8.7213(1)	8.9170(1)	8.7258(1)	8.8369(1)
c [Å]	35.055(3)	12.4729(1)	12.2858(1)	12.6978(2)	18.7268(3)
α [°]	90	90	90	90	83.5551(5)
β [°]	103.317(3)	99.8106(4)	93.1878(5)	104.9695(7)	82.0931(5)
γ [°]	90	90	90	90	78.4925(9)
V [Å ³]	13401.1(15)	2008.38	2021.10(3)	1968.33(5)	990.86(3)
Z	24	4	4	4	2
D _{calcd.} [g cm ⁻³]	1.716	1.832	2.136	1.853	1.907
μ [mm ⁻¹]	6.442	7.132	8.608	7.274	7.235
Abs. corr.	multi-scan	multi-scan	multi-scan	multi-scan	analytical
Abs. corr. range	0.50–0.94	0.10–0.17	0.19–0.46	0.41–0.65	0.09–0.71
(sin θ/λ) _{max} [Å ⁻¹]	0.61	0.65	0.65	0.65	0.65
Refl. (meas./unique)	137812/12469	35146/4599	41849/4637	29469/4519	18904/4499
Param./restraints	807/66	240/0	230/0	239/0	248/0
R1/wR2 [$I > 2\sigma(I)$]	0.0250/0.0505	0.0162/0.0350	0.0204/0.0493	0.0215/0.0407	0.0197/0.0449
R1/wR2 [all refl.]	0.0395/0.0550	0.0188/0.0357	0.0236/0.0589	0.0319/0.0433	0.0217/0.0460
S	1.022	1.086	1.129	1.052	1.086

tary crystallographic data for this paper. These data can be obtained free of charge from The Cambridge Crystallographic Data Centre via www.ccdc.cam.ac.uk/data_request/cif.

Supporting Information (see footnote on the first page of this article): Results of the BLA calculations (Table S1) and a Quaternion fit of the two ordered molecules in the crystal structure of **1** (Figure S1).

Acknowledgments

This work was partially supported (G. D. B., M. L. and A. L. S.) by the Council for Chemical Sciences of the Netherlands Organization for Scientific Research (NWO/CW). Duncan M. Tooke is acknowledged for collecting the X-ray data of compound **1**. J. G. thanks the Junta de Comunidades de Castilla-La Mancha for a grant.

- [1] H. Meier, *Angew. Chem. Int. Ed.* **2005**, *44*, 2482–2506.
- [2] D. R. Kanis, M. A. Ratner, T. J. Marks, *Chem. Rev.* **1994**, *94*, 195–242.
- [3] R. H. Friend, R. W. Gymer, A. B. Holmes, J. H. Burroughes, R. N. Marks, C. Taliani, D. D. C. Bradley, D. A. Dos Santos, J. L. Brédas, M. Lögdlund, W. R. Salaneck, *Nature* **1999**, *397*, 121–128.
- [4] A. Dulcic, C. Flytzanis, C. L. Tang, D. Pépin, M. Fétizon, Y. Hoppilliard, *J. Chem. Phys.* **1981**, *74*, 1559–1563.
- [5] H. Meier, *Angew. Chem. Int. Ed. Engl.* **1992**, *31*, 1399–1420.
- [6] D. H. Waldeck, *Chem. Rev.* **1991**, *91*, 415–436.
- [7] V. Papper, G. I. Likhtenshtein, *J. Photochem. Photobiol., A* **2001**, *140*, 39–52.
- [8] V. Papper, D. Pines, G. Likhtenshtein, E. Pines, *J. Photochem. Photobiol., A* **1997**, *111*, 87–96.
- [9] S. K. Hurst, M. G. Humphrey, T. Isoshima, K. Wostyn, I. Asselberghs, K. Clays, A. Persoons, M. Samoc, B. Luther-Davies, *Organometallics* **2002**, *21*, 2024–2026.
- [10] H. Lang, R. Packheiser, B. Walfort, *Organometallics* **2006**, *25*, 1836–1850.

- [11] A. J. Sandee, C. K. Williams, N. R. Evans, J. E. Davies, C. E. Boothby, A. Köhler, R. H. Friend, A. B. Holmes, *J. Am. Chem. Soc.* **2004**, *126*, 7041–7048.
- [12] J. Vicente, M. T. Chicote, M. D. Abrisqueta, M. C. R. de Arellano, P. G. Jones, M. G. Humphrey, M. P. Cifuentes, M. Samoc, B. Luther-Davies, *Organometallics* **2000**, *19*, 2968–2974.
- [13] I. R. Whittall, M. G. Humphrey, A. Persoons, S. Houbrechts, *Organometallics* **1996**, *15*, 1935–1941.
- [14] I. Asselberghs, K. Clays, A. Persoons, A. M. McDonagh, M. D. Ward, J. A. McCleverty, *Chem. Phys. Lett.* **2003**, *368*, 408–411.
- [15] B. J. Coe, C. J. Jones, J. A. McCleverty, D. Bloor, G. Cross, *J. Organomet. Chem.* **1994**, *464*, 225–232.
- [16] M. Malaun, R. Kowallick, A. M. McDonagh, M. Marcaccio, R. L. Paul, I. Asselberghs, K. Clays, A. Persoons, B. Bildstein, C. Fiorini, J. M. Nunzi, M. D. Ward, J. A. McCleverty, *J. Chem. Soc., Dalton Trans.* **2001**, 3025–3038.
- [17] M. Marcaccio, J. A. McCleverty, W. Akemann, C. Fiorini-Debuisschert, J. M. Nunzi, *J. Photochem. Photobiol., A* **2004**, *163*, 413–417.
- [18] S. Back, M. Albrecht, A. L. Spek, G. Rheinwald, H. Lang, G. van Koten, *Organometallics* **2001**, *20*, 1024–1027.
- [19] S. Back, R. A. Gossage, H. Lang, G. van Koten, *Eur. J. Inorg. Chem.* **2000**, 1457–1464.
- [20] S. Back, M. Lutz, A. L. Spek, H. Lang, G. van Koten, *J. Organomet. Chem.* **2001**, *620*, 227–234.
- [21] S. L. James, G. Verspui, A. L. Spek, G. van Koten, *Chem. Commun.* **1996**, 1309–1310.
- [22] M. Gagliardo, G. Rodríguez, H. H. Dam, M. Lutz, A. L. Spek, R. W. A. Havenith, P. Coppo, L. De Cola, F. Hartl, G. P. M. van Klink, G. van Koten, *Inorg. Chem.* **2006**, *45*, 2143–2155.
- [23] M. Q. Slagt, G. Rodríguez, M. M. P. Grutters, R. J. M. Klein Gebbink, W. Klopper, L. W. Jenneskens, M. Lutz, A. L. Spek, G. van Koten, *Chem. Eur. J.* **2004**, *10*, 1331–1344.
- [24] L. A. van de Kuil, H. Luitjes, D. M. Grove, J. W. Zwikker, J. G. M. van der Linden, A. M. Roelofsen, L. W. Jenneskens, W. Drenth, G. van Koten, *Organometallics* **1994**, *13*, 468–477.
- [25] C. Hansch, A. Leo, R. W. Taft, *Chem. Rev.* **1991**, *91*, 165–195.
- [26] S. J. Farley, D. L. Rochester, A. L. Thompson, J. A. K. Howard, J. A. G. Williams, *Inorg. Chem.* **2005**, *44*, 9690–9703.

- [27] W. Lu, B. X. Mi, M. C. W. Chan, Z. Hui, N. Y. Zhu, S. T. Lee, C. M. Che, *Chem. Commun.* **2002**, 206–207.
- [28] M. Maestri, C. Deuschel-Cornioley, A. von Zelewsky, *Coord. Chem. Rev.* **1991**, *111*, 117–123.
- [29] H. Jude, J. A. K. Bauer, W. B. Connick, *Inorg. Chem.* **2002**, *41*, 2275–2281.
- [30] H. Jude, J. A. K. Bauer, W. B. Connick, *Inorg. Chem.* **2004**, *43*, 725–733.
- [31] H. Jude, J. A. K. Bauer, W. B. Connick, *Inorg. Chem.* **2005**, *44*, 1211–1220.
- [32] T. Kanbara, K. Okada, T. Yamamoto, H. Ogawa, T. Inoue, *J. Organomet. Chem.* **2004**, *689*, 1860–1864.
- [33] I. O. Donkor, T. L. Huang, B. Tao, D. Rattendi, S. Lane, M. Vargas, B. Goldberg, C. Bacchi, *J. Med. Chem.* **2003**, *46*, 1041–1048.
- [34] T. L. Huang, Q. Zhang, A. T. White, S. F. Queener, M. S. Bartlett, J. W. Smith, I. O. Donkor, *Bioorg. Med. Chem. Lett.* **1996**, *6*, 2087–2090.
- [35] J. L. H. Jiwan, J. P. Soumillion, *J. Phys. Chem.* **1995**, *99*, 14223–14230.
- [36] E. Peeters, P. A. van Hal, S. C. J. Meskers, R. A. J. Janssen, E. W. Meijer, *Chem. Eur. J.* **2002**, *8*, 4470–4474.
- [37] S. D. Taylor, C. C. Kotoris, A. N. Dinaut, M. J. Chen, *Tetrahedron* **1998**, *54*, 1691–1714.
- [38] R. Wigglesworth, C. S. J. Walpole, S. Bevan, E. A. Campbell, A. Dray, G. A. Hughes, I. James, K. J. Masdin, J. Winter, *J. Med. Chem.* **1996**, *39*, 4942–4951.
- [39] C. H. M. Amijs, G. P. M. van Klink, G. van Koten, *Green Chem.* **2003**, *5*, 470–474.
- [40] M. R. Pitts, J. R. Harrison, C. J. Moody, *J. Chem. Soc., Perkin Trans. 1* **2001**, 955–977.
- [41] G. Brizius, N. G. Pschirer, W. Steffen, K. Stitzer, H. C. zur Loye, U. H. F. Bunz, *J. Am. Chem. Soc.* **2000**, *122*, 12435–12440.
- [42] E. Diez-Barra, J. C. Garcia-Martinez, S. Merino, R. del Rey, J. Rodriguez-Lopez, P. Sanchez-Verdu, J. Tejada, *J. Org. Chem.* **2001**, *66*, 5664–5670.
- [43] H. Meier, J. Gerold, H. Kolshorn, B. Muhling, *Chem. Eur. J.* **2004**, *10*, 360–370.
- [44] K. R. J. Thomas, J. T. Lin, K. J. Lin, *Organometallics* **1999**, *18*, 5285–5291.
- [45] J. Harada, K. Ogawa, *J. Am. Chem. Soc.* **2004**, *126*, 3539–3544.
- [46] M. Albrecht, B. M. Kocks, A. L. Spek, G. van Koten, *J. Organomet. Chem.* **2001**, *624*, 271–286.
- [47] M. Albrecht, M. Lutz, A. M. M. Schreurs, E. T. H. Lutz, A. L. Spek, G. van Koten, *J. Chem. Soc., Dalton Trans.* **2000**, 3797–3804.
- [48] A. V. Chuchuryukin, P. A. Chase, H. P. Dijkstra, B. M. J. M. Suijkerbuijk, A. M. Mills, A. L. Spek, G. P. M. van Klink, G. van Koten, *Adv. Synth. Catal.* **2005**, *347*, 447–462.
- [49] J. G. Donkervoort, J. L. Vicario, J. T. B. H. Jastrzebski, W. J. J. Smeets, A. L. Spek, G. van Koten, *J. Organomet. Chem.* **1998**, *551*, 1–7.
- [50] E. A. S. Bustamante, T. Hanemann, W. Haase, I. Svoboda, H. Fuess, *Acta Crystallogr., Sect. C: Cryst. Struct. Commun.* **1995**, *51*, 2192–2196.
- [51] D. C. R. Hockless, I. R. Whittall, M. G. Humphrey, *Acta Crystallogr., Sect. C: Cryst. Struct. Commun.* **1996**, *52*, 3222–3224.
- [52] J. Catalan, *Chem. Phys. Lett.* **2006**, *421*, 134–137.
- [53] S. P. Kwasniewski, L. Claes, J. P. Francois, M. S. Deleuze, *J. Chem. Phys.* **2003**, *118*, 7823–7836.
- [54] Z. H. Yu, L. T. Li, W. Fu, L. P. Li, *J. Phys. Chem. A* **1998**, *102*, 2016–2028.
- [55] C. H. Choi, M. Kertesz, *J. Phys. Chem. A* **1997**, *101*, 3823–3831.
- [56] C. J. Finder, M. G. Newton, N. L. Allinger, *Acta Crystallographica Sect. B: Struct. Sci.* **1974**, *B30*, 411–415.
- [57] M. Traetteberg, E. B. Frantsen, F. C. Mijlhoff, A. Hoekstra, *J. Mol. Struct.* **1975**, *26*, 57–68.
- [58] J. A. Bouwstra, A. Schouten, J. Kroon, *Acta Crystallographica Sect. C: Cryst. Struct. Communications* **1984**, *C40*, 428–431.
- [59] Z. Q. Liu, Q. Fang, D. Wang, D. X. Cao, G. Xue, W. T. Yu, H. Lei, *Chem. Eur. J.* **2003**, *9*, 5074–5084.
- [60] J. S. Yang, Y. H. Lin, C. S. Yang, *Org. Lett.* **2002**, *4*, 777–780.
- [61] S. K. Hurst, M. P. Cifuentes, J. P. L. Morrall, N. T. Lucas, I. R. Whittall, M. G. Humphrey, I. Asselberghs, A. Persoons, M. Samoc, B. Luther-Davies, A. C. Willis, *Organometallics* **2001**, *20*, 4664–4675.
- [62] T. M. Gilbert, F. J. Hadley, C. B. Bauer, R. D. Rogers, *Organometallics* **1994**, *13*, 2024–2034.
- [63] A. Hilger, J. P. Gisselbrecht, R. R. Tykwinski, C. Boudon, M. Schreiber, R. E. Martin, H. P. Luthi, M. Gross, F. Diederich, *J. Am. Chem. Soc.* **1997**, *119*, 2069–2078.
- [64] T. Michinobu, J. C. May, J. H. Lim, C. Boudon, J. P. Gisselbrecht, P. Seiler, M. Gross, I. Biaggio, F. Diederich, *Chem. Commun.* **2005**, 737–739.
- [65] See the supporting information for the exact assignment of the bonds and the bond length alternation calculations.
- [66] C. A. van Walree, A. W. Maarsman, A. W. Marsman, M. C. Flipse, L. W. Jenneskens, W. J. J. Smeets, A. L. Spek, *J. Chem. Soc., Perkin Trans. 2* **1997**, 809–819.
- [67] R. Frantz, J. O. Durand, G. F. Lanneau, *J. Organomet. Chem.* **2004**, *689*, 1867–1871.
- [68] J. Mason, *Chem. Rev.* **1987**, *87*, 1299–1313.
- [69] B. Yin, F. Niemeyer, J. A. G. Williams, J. Jiang, A. Boucekkine, L. Toupet, H. Le Bozec, V. Guerschais, *Inorg. Chem.* **2006**, *45*, 8584–8596.
- [70] C. A. van Walree, O. Franssen, A. W. Marsman, M. C. Flipse, L. W. Jenneskens, *J. Chem. Soc., Perkin Trans. 2* **1997**, 799–807.
- [71] L. T. Cheng, W. Tam, S. H. Stevenson, G. R. Meredith, G. Rikken, S. R. Marder, *J. Phys. Chem.* **1991**, *95*, 10631–10643.
- [72] H. Gruen, H. Görner, *J. Phys. Chem.* **1989**, *93*, 7144–7152.
- [73] Values for ϵ and n were taken from: C. Reichardt, *Solvents and Solvent Effects in Organic Chemistry*, 2nd ed., VCH, Weinheim **1988**.
- [74] E. Lippert, *Z. Naturforsch., A: Phys. Sci.* **1955**, *10*, 541–546.
- [75] Y. V. Il'ichev, W. Kühnle, K. A. Zachariasse, *Chem. Phys.* **1996**, *211*, 441–453.
- [76] A. Kowski, *Z. Naturforsch., A: Phys. Sci.* **2002**, *57*, 255–262.
- [77] The Onsager radius was obtained out of the unit cell volume after it was normalized by using the K. P. I. correction; for **6**: $\rho = 4.363$ Å, for **7**: $\rho = 4.391$ Å.
- [78] I. Majerz, A. Koll, *Acta Crystallogr., Sect. B: Struct. Sci.* **2004**, *60*, 406–415.
- [79] R. Lapouyade, A. Kuhn, J. F. Létard, W. Rettig, *Chem. Phys. Lett.* **1993**, *208*, 48–58.
- [80] R. Lapouyade, K. Czeschka, W. Majenz, W. Rettig, E. Gilabert, C. Rullière, *J. Phys. Chem.* **1992**, *96*, 9643–9650.
- [81] H. LeBreton, B. Bennetau, J. F. Létard, R. Lapouyade, W. Rettig, *J. Photochem. Photobiol., A* **1996**, *95*, 7–20.
- [82] J. F. Létard, R. Lapouyade, W. Rettig, *Chem. Phys. Lett.* **1994**, *222*, 209–216.
- [83] D. Pines, E. Pines, W. Rettig, *J. Phys. Chem. A* **2003**, *107*, 236–242.
- [84] K. Rechthaler, G. Köhler, *Chem. Phys. Lett.* **1996**, *250*, 152–158.
- [85] W. Rettig, W. Majenz, *Chem. Phys. Lett.* **1989**, *154*, 335–341.
- [86] W. Rettig, W. Majenz, R. Herter, J. F. Létard, R. Lapouyade, *Pure Appl. Chem.* **1993**, *65*, 1699–1704.
- [87] J. F. Létard, R. Lapouyade, W. Rettig, *Chem. Phys.* **1994**, *186*, 119–131.
- [88] A. J. Canty, J. Patel, B. W. Skelton, A. H. White, *J. Organomet. Chem.* **2000**, *599*, 195–199.
- [89] B. R. Steele, K. Vrieze, *Transition Met. Chem.* **1977**, *2*, 140–144.
- [90] G. Rodriguez, M. Albrecht, J. Schoenmaker, A. Ford, M. Lutz, A. L. Spek, G. van Koten, *J. Am. Chem. Soc.* **2002**, *124*, 5127–5138.
- [91] S. M. Moerlein, *J. Organomet. Chem.* **1987**, *319*, 29–39.

- [92] P. S. Pregosin, *Coord. Chem. Rev.* **1982**, *44*, 247–291.
- [93] D. F. Eaton, *Pure Appl. Chem.* **1988**, *60*, 1107–1114.
- [94] P. T. Beurskens, G. Admiraal, G. Beurskens, W. P. Bosman, S. Garcia-Granda, R. O. Gould, J. M. M. Smits, C. Smykalla, *The DIRDIF99 Program System – Technical Report of the Crystallography Laboratory*, University of Nijmegen, The Netherlands, **1999**.
- [95] G. M. Sheldrick, *SHELXL-97: Program for Crystal Structure Refinement*, University of Göttingen, Germany, **1997**.
- [96] A. L. Spek, *J. Appl. Crystallogr.* **2003**, *36*, 7–13.

Received: November 17, 2006
Published Online: February 23, 2007